Broadband Topological Slow Light through Brillouin Zone Winding

Sander A. Mann[1] and Andrea Alù[1,2,3,*]

[1]Photonics Initiative, Advanced Science Research Center, City University of New York, New York, New York 10031, USA
[2]Department of Electrical Engineering, City College of The City University of New York, New York, New York 10031, USA
[3]Physics Program, Graduate Center, City University of New York, New York, New York 10016, USA

(Received 20 January 2021; accepted 5 August 2021; published 13 September 2021)

Topological photonic insulators have attracted significant attention for their robust transport of light, impervious to scattering and disorder. This feature is ideally suited for slow light applications, which are typically limited by disorder-induced attenuation. However, no practical approach to broadband topologically protected slow light has been demonstrated yet. In this work, we achieve slow light in topologically unidirectional waveguides based on periodically loading an edge termination with suitably tailored resonances. The resulting edge state dispersion can wind around the Brillouin zone multiple times sustaining broadband, topologically robust slow light, opening exciting opportunities in various photonic scenarios.

DOI: 10.1103/PhysRevLett.127.123601

The interaction between light and matter can be considerably increased by structuring materials on the scale of the wavelength. One attractive avenue is to structure materials so that the group velocity of light is significantly reduced [1,2]. Because of its low velocity, slow light goes hand in hand with large field intensities and can therefore be used to enhance light-matter interactions and nonlinear phenomena [3–8]. In addition, slow light enables the miniaturization of optical devices, as in the case of optical buffers [9–11]. Impressive results in this context have been achieved in photonic crystal line-defect waveguides [12,13] and coupled resonator optical waveguides (CROWs) [14–17]. However, these slow light devices are ultimately practically limited by the fact that low group velocities also imply extreme sensitivity to imperfections, leading to losses induced by backscattering and localization phenomena [18–21].

The field of topological photonics may provide a solution to this challenge [22]. Inspired by developments in solid-state topological insulators, in which the inherent robustness of the Hall conductance was shown to be related to a topological invariant, the Chern number, Haldane and Raghu showed that nontrivial topological bands can also arise for classical electromagnetic waves in periodic media with broken time-reversal symmetry [23,24]. The most striking consequence of this effect is that chiral, unidirectional edge states must arise at the interface between photonic materials with different Chern numbers [25], and these edge states are topologically protected against disorder [26–28]. As a result, it has been speculated that these unidirectional edge states make photonic topological insulators an ideal platform to address the current challenges of slow light devices (see, e.g., Refs. [26,27,29–36] for a selection). However, despite these suggestions, broadband, topologically protected slow light has not yet been demonstrated.

Several different photonic topological phases have been unveiled since the seminal work by Raghu and Haldane. In particular, photonic structures supporting phenomena analogous to the quantum spin Hall effect have been recently introduced [30,37–39]. Despite being reciprocal, they exhibit helical edge states topologically protected against certain types of disorder, enabling more robust slow light phenomena [30]. However, given that time-reversal symmetry in these systems requires the existence of a backward propagating edge state, for truly random disorder that couples the helicity of forward and backward waves, these slow helical edge states are ultimately expected to succumb as well [40].

Here, we study chiral edge states in systems with broken time-reversal symmetry. It has recently been proposed, based on the Haldane model of a honeycomb lattice, that broadband slow light may possibly be achieved by winding the edge state dispersion around the Brillouin zone multiple times [34]. However, the approach taken in Ref. [34] does not directly translate into a realistic photonic setting. We explore a practical approach to achieve Brillouin zone winding, based on periodically loading the edge with resonators [41]. We show that the approach is versatile, readily achieves large delays, and is straightforward to implement in multiple different ways.

Consider a waveguide side coupled to a periodic arrangement of resonators with period Λ. Using coupled-mode theory, the equation of motion for the nth set of resonances is [42,43]

$$\frac{d}{dt}\mathbf{a}_n = (i\Omega - \Gamma)\mathbf{a}_n + \mathbf{K}^{\mathrm{T}}\mathbf{s}_n^{(+)}, \tag{1}$$

where Ω is a Hermitian matrix containing the center frequencies and evanescent coupling between on-site

 © 2021 American Physical Society

resonances, Γ is a matrix containing the loss rates and dissipative coupling rates, and $\mathbf{K}$ is the coupling coefficient between the waveguide and the resonances. The modal amplitude is normalized so that the stored energy in $a_{n,i}$ is given by $|a_{n,i}|^2$. The amplitude of the outgoing waveguide modes obeys

$$\mathbf{s}_n^{(-)} = \mathbf{C}\mathbf{s}_n^{(+)} + \mathbf{D}\mathbf{a}_n, \tag{2}$$

where $\mathbf{C}$ is the direct scattering matrix (in the absence of resonances), and it is determined by the bare waveguide propagation constant k_w and unit cell length d, $\mathbf{C} = e^{-ik_w\Lambda}\left(\begin{smallmatrix}0 & 1\\ 1 & 0\end{smallmatrix}\right)$, and $\mathbf{D}$ is the coupling matrix between the resonators and the outgoing waveguide modes. Because of Bloch's theorem, neighboring unit cells are related as $\mathbf{a}_{n+1} = e^{-ik_x\Lambda}\mathbf{a}_n$, where k_x is the propagation constant of the combined system of waveguide and resonances. Combining Bloch's theorem with Eqs. (1),(2) and the coupled-mode theory identities [42,44] enables us to calculate the dispersion relation [43].

As an instructive example, Fig. 1 shows the dispersion for waveguides coupled to a single symmetric resonance per unit cell. If the bare waveguide is reciprocal [Fig. 1(a)], it supports both a forward and backward mode (shown by the gray dashed lines). The resonance will couple to both forward and backward propagating modes, and due to Bragg diffraction a band gap opens near the resonance center frequency, at which the resonance reflects most strongly. The group velocity just outside the band gap is low, and it vanishes exactly at the band edge. This regime has been commonly used for slow light applications [2,10], but they are generally dispersive and narrow band and, more importantly, they are susceptible to disorder, limiting the lowest achievable group velocity.

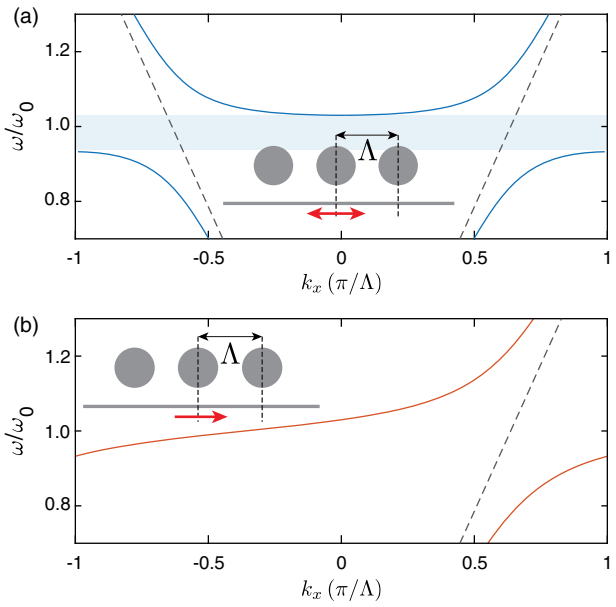

FIG. 1. (a) Dispersion of a bare reciprocal waveguide (gray dashed lines), and a reciprocal waveguide side-coupled to a periodic array of resonances (blue, see inset for schematic). Near the center frequency a band gap opens, and on both sides of the gap narrowband and dispersive regions supporting slow light arise. (b) If the bare waveguide instead is nonreciprocal and unidirectional, so that only a forward mode is supported (gray dashed line), no band gap opens when the waveguide is coupled to the same periodic cavity array (see inset). A region of slow light arises at the resonance center frequency. Dispersion calculated with Eqs. (1),(2).

The dispersion becomes markedly different if we consider a nonreciprocal and unidirectional waveguide, such as the edge state in a photonic topological insulator with broken time-reversal symmetry. In this case, in order to calculate the dispersion we need to use nonreciprocal coupled-mode theory [43]. The bare dispersion for a waveguide that supports only a forward mode is shown in Fig. 1(b) by the single gray dashed line. Introducing the same periodic arrangement of resonances as in Fig. 1(a) (solid orange line) does not result in a band gap any longer. Instead, the dispersion wraps around the Brillouin zone one time, resulting in a reduced group velocity over the bandwidth of the resonance, as evidenced by the slope of the dispersion curve. Interestingly, this dispersion is identical to the forward dispersion of a reciprocal side-coupled integrated spaced sequenced of ring resonators (SCISSOR) [45,46]. This is because the (anti-)clockwise modes in a ring resonator couple only to the forward or backward modes, due to momentum conservation. However, fabrication imperfections couple the (anti-)clockwise modes and induce standing modes that decay into both forward and backward propagating waves, resulting in a situation similar to Fig. 1(a). Hence, while the ideal dispersion is identical, unidirectionality is required to enable a robust practical implementation.

Intuitively, the dispersion in Fig. 1(b) can be understood by considering that the difference in transmission phase at frequencies far above and below a resonance is 2π. Adding a resonance in each unit cell thus implies that there is an additional 2π phase difference between frequencies above and below the resonance, which in the periodic arrangement thus implies that the dispersion must traverse an additional $2\pi/\Lambda$ for each resonance in the unit cell. In the Brillouin zone, this appears as a single wrapping around the zone (as the dispersion runs form $-\pi/\Lambda$ to π/Λ). In other words, the number of resonances per unit cell that the edge termination supports is directly related to the number of times the dispersion wraps around the Brillouin zone. We can verify this argument using the framework presented earlier: Fig. 2(a) schematically shows a unidirectional waveguide side coupled to a resonator, which in turn is evanescently coupled to additional resonators. The dispersion for up to four resonances per unit cell calculated using Eqs. (1),(2) is shown in Figs. 2(b),2(c). As expected, the dispersion winds around the Brillouin zone one

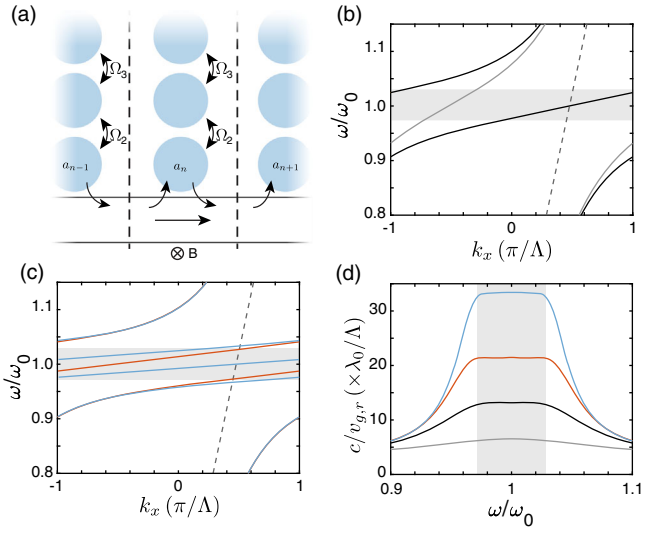

FIG. 2. (a) Schematic of a unidirectional waveguide (due to, e.g., a static magnetic induction bias B) side coupled to a periodic array of resonant cavities. (b) Dispersion of the bare waveguide (gray dashed line), and loaded with one (gray) and two (black) cavities per unit period. The waveguide is designed to support slow light in the gray shaded region. (c) Same as in (b), but now with three (orange) and four (blue) loading cavities. For each additional resonance, the dispersion wraps around the Brillouin zone once more. (d) Impact on the group velocity of adding resonances. The curves are normalized by a factor λ_0/Λ: a small period decreases the net group velocity. All results in this figure are calculated using the coupled-mode theory framework.

additional time for each additional resonance. Since the bandwidth remains the same, the increased winding results in slower group velocities over the entire bandwidth, enabling broadband slow light [34].

In analyzing the group velocity, we can distinguish between the contribution of the resonance loading v_{gr}, and of the bare waveguide v_{gw}: $c/v_g = c/v_{gw} + c/v_{gr}$, where c is the speed of light in vacuum. The factor c/v_{gr} is shown in Fig. 2(d) for the dispersion curves in Figs. 2(b),2(c). As expected, as more resonances are added the group velocity further decreases. With four coupled resonances, for example, c/v_{gr} reaches approximately $35\lambda_0/\Lambda$, where λ_0 is the center wavelength and Λ is the unit cell size, over a bandwidth of approximately $\omega_0/20$. In order to minimize distortion as a slow light pulse travels along the edge, higher-order derivatives of the group velocity should ideally vanish within the operating bandwidth. In a regular CROW, a flat top dispersion is challenging to obtain [47]; however, as shown in Fig. 2(d), side-coupled chains of resonators support flat top dispersion over a wide bandwidth [43], indicating that this resonant edge termination is an ideal candidate for topologically robust slow light.

To demonstrate a practical implementation of this concept, we consider a two-dimensional photonic crystal consisting of a square lattice of yttrium-iron-garnett (YIG) rods, based on Ref. [26], numerically calculated using COMSOL Multiphysics. The rods have a radius of $0.11\Lambda_0$, where Λ_0 is the crystal period. This photonic crystal supports a quadratic degeneracy at the M point, between the 2nd and 3rd band, which is lifted when an out-of-plane magnetic bias is applied. Operating at 4.28 GHz and neglecting dispersion and losses, the YIG permittivity is $\varepsilon = 15\varepsilon_0$ and, with a 0.16 T stationary magnetic bias in the out-of-plane direction the permeability tensor is [26,48]

$$\boldsymbol{\mu} = \mu_0 \begin{pmatrix} 14 & 12.4i & 0 \\ -12.4i & 14 & 0 \\ 0 & 0 & 1 \end{pmatrix}. \tag{3}$$

The resulting band diagram projected on the x direction is shown in Fig. 3(a). The topological invariant of the nth band can be calculated through its Berry curvature $\Omega_n(\mathbf{k}) = i(\langle\delta_{k_x}E_{n,\mathbf{k}}|\delta_{k_y}E_{n,\mathbf{k}}\rangle - \langle\delta_{k_y}E_{n,\mathbf{k}}|\delta_{k_x}E_{n,\mathbf{k}}\rangle)$, where $E_{n,\mathbf{k}}$ is the corresponding field profile [22]. The Chern number, shown next to each band in Fig. 3(a), is then given by the integral of the Berry curvature over the Brillouin zone, $C_n = 1/2\pi \int_{\mathrm{BZ}} d\mathbf{k}\Omega_n(\mathbf{k})$.

When the photonic topological insulator is interfaced with a topologically trivial opaque material, such as a

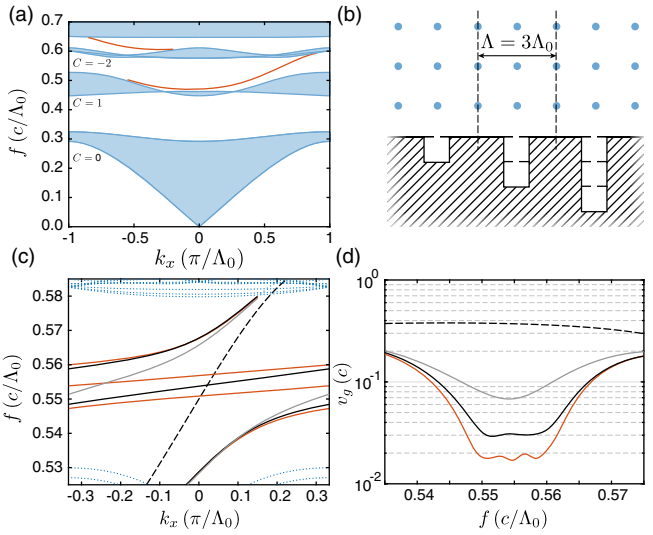

FIG. 3. (a) Dispersion of the YIG photonic crystal, with Chern numbers shown on the left. The red lines are topologically protected nonreciprocal edge states. (b) Schematic of the edge terminations considered here: configurations containing up to three rectangular cavities, with supercell denoted by dashed lines. (c) Dispersion of the edge state with one (gray), two (black), and three (orange) cavities, showing increasing band folding. (d) Group velocity of the edge state across the nontrivial band gap with one (gray), two (black), or three (orange) cavities. The gray dashed line shows the group velocity of the bare edge state. All results in this figure are calculated using COMSOL Multiphysics.

perfect electric conductor (PEC), a topological phase transition must occur, which yields unidirectional edge states crossing the gap. The number and direction of edge states in a topologically nontrivial band gap is given by the sum over all band Chern numbers below the gap, stemming from the bulk-edge correspondence [25]. For our photonic crystal, this principle predicts one edge state in both the 2nd and 3rd gap, with opposite direction, as confirmed by the red curves in Fig. 3(a).

We focus on the 2nd gap, with a fractional bandwidth of 10%. To slow down the edge state we introduce a rectangular resonator in the PEC wall, interfaced with the edge state through an aperture [Fig. 3(b)]. Such a resonator supports a lowest-order resonance at $\varepsilon k_0^2 = (\pi/a)^2 + (\pi/b)^2$, where ε is the cavity relative permittivity, k_0 is the free-space wavenumber, a and b are the two rectangle dimensions. As a proof of principle, we repeat the resonator every three lattice constants, so that $\Lambda = 3\Lambda_0$. The individual resonator, not yet in a periodic array, has center frequency $\omega_0 = 0.555 \times 2\pi\Lambda_0/c$, designed so that it lies in the middle of the unidirectional gap. The loss rate $\gamma = 0.01\Lambda_0/c$ covers a significant portion of the gap, thereby enabling broadband slow light. The dispersion curves for the edge state without (dashed black) and with (gray) the resonator loading are shown in Fig. 3(c). As expected, the forward dispersion clearly wraps around the Brillouin zone, slowing down edge state propagation across the gap.

To further slow the edge state, we introduce an additional resonator in the unit cell, coupled to the bottom of the resonant cavity through an aperture [see Fig. 3(b)]. The dispersion in the case of a double cavity load is also shown in Fig. 3(c), and as expected the introduction of an additional resonance causes the dispersion to wrap around the Brillouin zone one additional time. Introducing a third resonator, coupled to the second resonator via a similar aperture, also shown in Fig. 3(b), causes the dispersion to wrap around the Brillouin zone once more.

The group velocity of these different resonant terminations is calculated in Fig. 3(d). In agreement with Fig. 2(d), the bandwidth remains more or less identical, while the group velocity is significantly reduced as each resonator is added. If we define the slow light bandwidth as the frequency range with less than 10% variation in group index, the system with three resonators per unit cell obtains an average group index $n_g = 55$ over a fractional bandwidth of 1.9%. This yields a group index-bandwidth product (GBP) of 1.05 [47], which is considerable relative to existing slow light designs. Caution must be taken in directly comparing this GBP to slow light waveguides in silicon slab photonic crystals, however: the use of PECs and the 2D nature of the considered geometry here are beneficial.

Having presented a practical approach to topologically protected slow light, in Fig. 4 we explore the additional benefit of these unidirectional slow light edge states: their

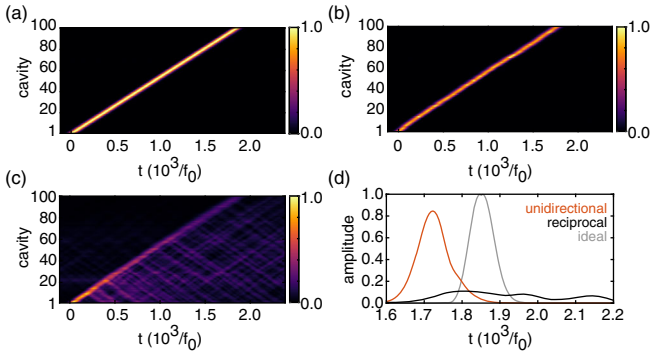

FIG. 4. (a) Propagation of a Gaussian pulse through a nonreciprocal unidirectional waveguide side coupled to three cavities per unit cell. In the ideal case, there is no difference between the reciprocal and nonreciprocal systems. (b) Propagation of the same pulse through the unidirectional system with a 1% relative standard deviation in each parameter. (c) The same as (b), but now in a reciprocal system. The clockwise and anticlockwise modes are assumed to be coupled by 1/25th of the largest intercavity coupling rate [43]. (d) The output pulses for the three scenarios shown. While there is some distortion in the unidirectional system with disorder, as expected, it vastly outperforms the reciprocal system. All results in this figure are calculated based on the coupled-mode theory framework.

expected robustness against disorder. Using the coupled-mode theory framework, we compare the propagation of a pulse with a $1/e^2$ width of $40/f_0$ along the edge with three cavities per unit cell, as considered in Fig. 2. First, the system is perfectly periodic [Fig. 4(a)], and the pulse propagates as expected, with little distortion due to the low group velocity dispersion. In Fig. 4(b), disorder is included: all system parameters have a Gaussian spread with relative standard deviation of 1%. This means that, for example, each of the cavities has a center frequency that lies within $\omega_0 \pm \omega_0/100$, where ω_0 is the ideal center frequency of that cavity and $\omega_0/100$ is the standard deviation of the distribution. Despite the disorder and low group velocity, the pulse largely maintains its shape over 100 unit cells. In contrast, in Fig. 4(c) we consider an equivalent reciprocal system, consisting of the aforementioned SCISSOR, with three ring resonators per unit cell. In the ideal scenario, the dispersion is identical to the unidirectional system; however, with disorder reflections arise and the pulse quickly disperses. Figure 4(d) shows the pulse shape at the end of the waveguide for each scenario, clearly highlighting the important advantages of topological slow light.

So far, we have focused on an implementation based on PEC cavities. The implementation of a resonant edge termination, however, is not limited to this approach, nor do the resonators need to be placed in the same location. The main requirement is that the configuration of resonators physically fits within a small enough propagation length to induce significant delay, which is why we

consider placing resonators along the transverse direction. An alternative approach, which may be more appropriate in systems where the topological insulator is interfaced with, e.g., a trivial photonic crystal instead of a low-loss metal, is to use photonic crystal cavities as loads. One may also directly add obstructions in the path of the edge state that can couple evanescently and form nonreciprocal Fabry-Perot resonances, as shown in Ref. [35]. We consider both of these approaches in Ref. [43].

Finally, we comment on the applicability of this approach to *helical* edge states in topological insulators that preserve time-reversal symmetry, analogous to the quantum spin Hall effect [38] or valley Hall effect [49–51]. As these systems are reciprocal, the edge states are bidirectional and therefore robust only against certain types of defects that do not couple opposite helicities. Even more importantly, the forward and backward propagating edge states are not orthogonal, resulting in a small gap arising when they cross [52]. As a result, winding the edge state around the Brillouin zone results in multiple small gaps opening and cannot lead to a continuous band of slow light with minimal group velocity dispersion as the one shown here. Implementing slow light based on Brillouin zone winding thus appears to require broken time-reversal symmetry, which at telecom frequencies can, e.g., be achieved using uniform temporal modulation [36].

To conclude, we have introduced an approach to create topologically protected slow light edge states, and analyzed its benefits for photonic applications. While topological protection has often been suggested as a means to protect slow light against disorder, an approach that can yield broadband protected slow light was still lacking. The proposed approach relies on loading the edge termination with an arrangement of resonators. Although many arrangements are possible, we have presented an approach based on a transverse array of loading resonators side-coupled to the topological edge state. For each added resonator, the dispersion winds an additional time around the Brillouin zone, increasing the slowdown factor. Additionally, we have demonstrated that in these unidirectional systems the impact of disorder is limited, making this approach to slow light very promising for various practical implementations and scenarios.

We acknowledge Professor Ewold Verhagen, Professor Dimitrios Sounas, and Dr. Michele Cotrufo for stimulating discussions. S. A. M. acknowledges a Rubicon fellowship from the Dutch Research Council (NWO). This work has been also supported by the Air Force Office of Scientific Research MURI program, a Vannevar Bush Faculty Fellowship and the Simons Foundation.

Note added.—During completion of this work we became aware of another work demonstrating topologically protected slow light through periodically loaded resonators [53].

*aalu@gc.cuny.edu

[1] T. F. Krauss, Nat. Photonics **2**, 448 (2008).
[2] T. Baba, Nat. Photonics **2**, 465 (2008).
[3] B. Corcoran, C. Monat, C. Grillet, D. J. Moss, B. J. Eggleton, T. P. White, L. O'Faolain, and T. F. Krauss, Nat. Photonics **3**, 206 (2009).
[4] J. F. McMillan, X. Yang, N. C. Panoiu, R. M. Osgood, and C. W. Wong, Opt. Lett. **31**, 1235 (2006).
[5] M. Soljačić, S. G. Johnson, S. Fan, M. Ibanescu, E. Ippen, and J. D. Joannopoulos, J. Opt. Soc. Am. B **19**, 2052 (2002).
[6] Y. Xu, R. K. Lee, and A. Yariv, J. Opt. Soc. Am. B **17**, 387 (2000).
[7] S. E. Harris and L. V. Hau, Phys. Rev. Lett. **82**, 4611 (1999).
[8] E. Verhagen, L. Kuipers, and A. Polman, Nano Lett. **7**, 334 (2007).
[9] R. S. Tucker, P. Ku, and C. J. Chang-hasnain, J. Lightwave Technol. **23**, 4046 (2005).
[10] M. L. Povinelli, S. G. Johnson, and J. D. Joannopoulos, Opt. Express **13**, 7145 (2005).
[11] D. A. B. Miller, Phys. Rev. Lett. **99**, 203903 (2007).
[12] Y. A. Vlasov, M. O'Boyle, H. F. Hamann, and S. J. McNab, Nature (London) **438**, 65 (2005).
[13] J. Li, T. P. White, L. O'Faolain, A. Gomez-Iglesias, and T. F. Krauss, Opt. Express **16**, 6227 (2008).
[14] N. Stefanou and A. Modinos, Phys. Rev. B **57**, 12127 (1998).
[15] A. Yariv, Y. Xu, R. K. Lee, and A. Scherer, Opt. Lett. **24**, 711 (1999).
[16] M. Notomi, E. Kuramochi, and T. Tanabe, Nat. Photonics **2**, 741 (2008).
[17] M. Minkov and V. Savona, Optica **2**, 631 (2015).
[18] S. Hughes, L. Ramunno, J. F. Young, and J. E. Sipe, Phys. Rev. Lett. **94**, 033903 (2005).
[19] A. Petrov, M. Krause, and M. Eich, Opt. Express **17**, 8676 (2009).
[20] S. Mazoyer, J. P. Hugonin, and P. Lalanne, Phys. Rev. Lett. **103**, 063903 (2009).
[21] R. J. P. Engelen, D. Mori, T. Baba, and L. Kuipers, Phys. Rev. Lett. **101**, 103901 (2008).
[22] T. Ozawa, H. M. Price, A. Amo, N. Goldman, M. Hafezi, L. Lu, M. C. Rechtsman, D. Schuster, J. Simon, O. Zilberberg, and I. Carusotto, Rev. Mod. Phys. **91**, 015006 (2019).
[23] F. D. M. Haldane and S. Raghu, Phys. Rev. Lett. **100**, 013904 (2008).
[24] S. Raghu and F. D. M. Haldane, Phys. Rev. A **78**, 033834 (2008).
[25] M. G. Silveirinha, Phys. Rev. X **9**, 011037 (2019).
[26] Z. Wang, Y. D. Chong, J. D. Joannopoulos, and M. Soljačić, Phys. Rev. Lett. **100**, 013905 (2008).
[27] Z. Wang, Y. Chong, J. D. Joannopoulos, and M. Soljačić, Nature (London) **461**, 772 (2009).
[28] M. C. Rechtsman, J. M. Zeuner, Y. Plotnik, Y. Lumer, D. Podolsky, F. Dreisow, S. Nolte, M. Segev, and A. Szameit, Nature (London) **496**, 196 (2013).
[29] L. Lu, J. D. Joannopoulos, and M. Soljačić, Nat. Photonics **8**, 821 (2014).
[30] M. Hafezi, E. A. Demler, M. D. Lukin, and J. M. Taylor, Nat. Phys. **7**, 907 (2011).
[31] Y. Yang, Y. Poo, R. Wu, Y. Gu, and P. Chen, Appl. Phys. Lett. **102**, 231113 (2013).

[32] K. Lai, T. Ma, X. Bo, S. Anlage, and G. Shvets, Sci. Rep. **6**, 28453 (2016).
[33] H. Yoshimi, T. Yamaguchi, Y. Ota, Y. Arakawa, and S. Iwamoto, Opt. Lett. **45**, 2648 (2020).
[34] J. Guglielmon and M. C. Rechtsman, Phys. Rev. Lett. **122**, 153904 (2019).
[35] S. A. Mann, D. L. Sounas, and A. Alù, Phys. Rev. B **100**, 020303(R) (2019).
[36] R. Duggan, S. A. Mann, and A. Alù, Phys. Rev. B **102**, 100303(R) (2020).
[37] M. Hafezi, S. Mittal, J. Fan, A. Migdall, and J. M. Taylor, Nat. Photonics **7**, 1001 (2013).
[38] L.-H. Wu and X. Hu, Phys. Rev. Lett. **114**, 223901 (2015).
[39] S. Barik, A. Karasahin, C. Flower, T. Cai, H. Miyake, W. DeGottardi, M. Hafezi, and E. Waks, Science **359**, 666 (2018).
[40] G. Arregui, J. Gomis-Bresco, C. M. Sotomayor-Torres, and P. D. Garcia, Phys. Rev. Lett. **126**, 027403 (2021).
[41] S. A. Mann and A. Alù, in *Proceedings of the Conference of Lasers Electro-Optics* (OSA Technical Digest, Washington, DC, 2020), p. JM4A.4.
[42] Wonjoo Suh, Zheng Wang, and Shanhui Fan, IEEE J. Quantum Electron. **40**, 1511 (2004).
[43] See Supplemental Material at http://link.aps.org/supplemental/10.1103/PhysRevLett.127.123601 for details on calculating the unidirectional dispersion, system parameters for the results shown in Figs. 2 and 3, the impact of absorption losses, and two other approaches to resonant edge terminations.
[44] S. A. Mann, D. L. Sounas, and A. Alù, Optica **6**, 104 (2019).
[45] J. E. Heebner, R. W. Boyd, and Q.-Han. Park, Phys. Rev. E **65**, 036619 (2002).
[46] J. B. Khurgin, Opt. Lett. **30**, 513 (2005).
[47] S. A. Schulz, L. O'Faolain, D. M. Beggs, T. P. White, A. Melloni, and T. F. Krauss, J. Opt. **12**, 104004 (2010).
[48] D. M. Pozar, *Microwave Engineering*, 4th ed. (Wiley, New York, 2012).
[49] T. Ma and G. Shvets, New J. Phys. **18**, 025012 (2016).
[50] A. B. Khanikaev, S. Hossein Mousavi, W. K. Tse, M. Kargarian, A. H. MacDonald, and G. Shvets, Nat. Mater. **12**, 233 (2013).
[51] X. Ni, D. Purtseladze, D. A. Smirnova, A. Slobozhanyuk, A. Alù, and A. B. Khanikaev, Sci. Adv. **4**, eaap8802 (2018).
[52] N. Parappurath, F. Alpeggiani, L. Kuipers, and E. Verhagen, Sci. Adv. **6**, eaaw4137 (2020).
[53] L. Yu, H. Xue, and B. Zhang, Appl. Phys. Lett. **118**, 071102 (2021).